Measurement of kaonic atoms at DAΦNE: what we can learn from their study

C. Curceanu (Petrascu)
Laboratori Nazionali di Frascati, LNF - INFN, Via E. Fermi 40, 00044 Frascati (Roma), Italy

1. – Introduction

The DAΦNE [1] electron-positron collider at the Frascati National Laboratories has made available a unique "beam" of negative kaons providing so unprecedented conditions for the study of the low-energy kaon-nucleon interaction, a field still largely unexplored.

The DEAR (DAΦNE Exotic Atom Research) experiment [2] at DAΦNE and its successor SIDDHARTA (SIlicon Drift Detector for Hadronic Atom Research by Timing Application) [3] aim at a precision measurement of the strong interaction shifts and widths of the fundamental $1s$ level, via the measurement of the x-ray transitions to this level, for kaonic hydrogen and kaonic deuterium. The aim is to extract the isospin dependent antikaon-nucleon scattering lengths and to contribute to the understanding of aspects of chiral symmetry breaking in the strangeness sector.

In practice, in studying kaonic hydrogen (deuterium) in order to measure the strong interaction component of the kaon-nucleon force, one measures the shift ϵ of the position of the K_α line ($2p \to 1s$ transition) from the one calculated from a purely electromagnetic interaction:

$$\epsilon = |E^{measured}_{2p\to 1s}| - |E^{e.m.}_{2p\to 1s}| \tag{1}$$

and the width (broadening) Γ of the $1s$ level given by the strong interaction, see Fig1.

The electromagnetic transition energy in kaonic hydrogen is calculated with 1 eV precision by solving the corresponding Klein-Gordon equation and applying the corrections for finite size and vacuum polarization. The resulting value is:

$$E^{e.m.}_{2p\to 1s} = (6480 \pm 1)\ eV \tag{2}$$

where the 1 eV error is dominated by the uncertainty of the kaon mass.

Until the advent of DAΦNE, the kaonic hydrogen parameters were measured at KEK [4], where the following results were found:

$$\epsilon = -323 \pm 63 \pm 11\ eV \tag{3}$$

$$\Gamma = 407 \pm 208 \pm 100\ eV \tag{4}$$

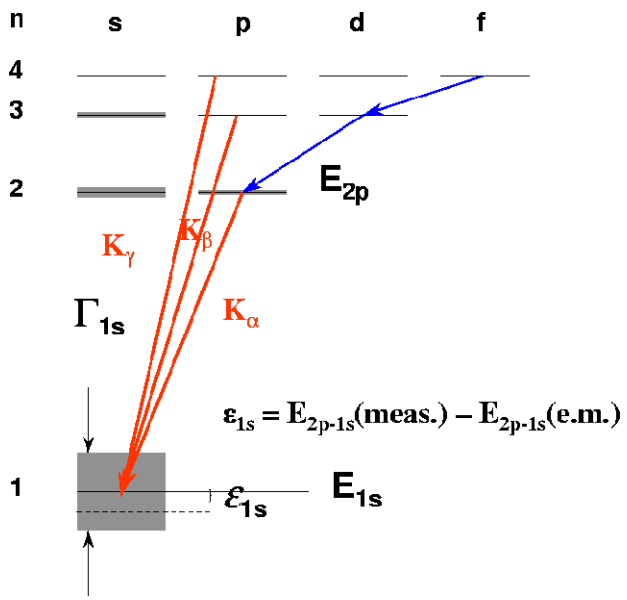

Fig. 1. – *The cascade process in kaonic atoms with the shift and the broadening of the* 1*s level, with respect to the purely electromagnetic calculated value, due to the presence of the strong interaction*

This measurement showed clearly that the antikaon-nucleon interaction is of repulsive type, but cannot be considered a precision measurement. The challenging aim of the DEAR/SIDDHARTA experiment is therefore to measure the kaonic hydrogen transition with a precision at the eV level. The kaonic deuterium will be measured for the first time. These results will represent a breakthrough in the study of the low-energy antikaon-nucleon interaction.

In Section 2, the physics of kaonic atoms is dealt with, while in Section 3 the low-energy kaon-nucleon phenomenology is introduced. Understanding low-energy strong interaction dynamics is the item briefly discussed in Section 4. The DEAR experimental setup installed at DAΦNE is presented in Section 5, while experimental results on kaonic atoms are reported in Section 6. The paper ends with the presentation of the coming experiment, SIDDHARTA, in Section 7, followed by Section 8 - Conclusions.

2. – The physics of kaonic atoms

A kaonic atom is formed whenever a negative kaon enters an atomic target, for instance hydrogen (deuterium), looses its kinetic energy through ionization and excitations of the medium atoms and molecules and is eventually captured in an excited orbit, replacing an electron. Various collisional cascade processes and radiative transitions deexcite the kaonic atom.

When the kaon reaches low-n states with small angular momentum, it is absorbed through the strong interaction with the nucleus. This strong interaction causes a shift in

the energies of the low-lying levels (essentially the $1s$ level) from their purely electromagnetic values, while the finite lifetime of the state is seen in an increase in the observed level width.

The shift ϵ and the width Γ of the $1s$ state of kaonic hydrogen are related to the real and imaginary part of the complex s-wave scattering length, a_{K^-p}. To the lowest order, neglecting isospin-breaking corrections, in the case of kaonic hydrogen these relations are given by the so-called Deser-Trueman formula [5]:

$$\epsilon + i\Gamma/2 = 2\alpha^3\mu^2 a_{K^-p} = (412\ eV\ fm^{-1}) \cdot a_{K^-p} \tag{5}$$

where α is the fine structure constant and μ the reduced mass of the K^-p system.

A similar relation applies to the case of kaonic deuterium and to the corresponding scattering length a_{K^-d}:

$$\epsilon + i\Gamma/2 = 2\alpha^3\mu^2 a_{K^-d} = (601\ eV\ fm^{-1}) \cdot a_{K^-d} \tag{6}$$

Recent results by using the non-relativistic effective Lagrangian approach to bound states have shown that the isospin-breaking corrections to the Deser relations might be important [6]. The main source is represented by the unitary cusp in the K^-p elastic amplitude. As far as Coulomb corrections are concerned, they are much smaller, remaining within a few percent.

Further investigations using effective field theories or lattice calculations to predict QCD amplitudes and compare with data from atomic spectra are needed [6, 7, 8]. See also W. Weise, this volume.

The observable scattering lengths a_{K^-p} and a_{K^-d} can be expressed in terms of the $\bar{K}N$ isospin dependent scattering lengths a_0 (I=0) and a_1 (I=1). The kaonic hydrogen scattering length is simply the average of the two:

$$a_{K^-p} = 1/2(a_0 + a_1) \tag{7}$$

while the kaonic deuterium scattering length a_{K^-d} is related to a_0 and a_1 in the following way:

$$a_{K^-d} = 2(\frac{m_N + m_K}{m_N + m_K/2})a^{(0)} + C \tag{8}$$

where

$$a^{(0)} = \frac{1}{2}(a_{K^-p} + a_{K^-n}) = \frac{1}{4}(3a_1 + a_0) \tag{9}$$

corresponds to the isoscalar $\bar{K}N$ scattering length. The first term in eq. (8) represents the lowest-order impulse approximation, i.e. K^- scattering from each (free) nucleon. The second term, C, includes all higher contributions related to the physics associated to the K^-d three-body interaction.

The determination of the $\bar{K}N$ scattering lengths requires the calculation of C. This is a well-known three-body problem, solvable by the use of Faddeev equations, when the two-body interactions are specified. The K^-d three-body problem includes the complication that the K^-p and K^-n interactions involve significant inelastic channels. The

K^-p and K^-n scattering lengths are thus complex and so is the K^-d scattering length. Incorporating $\bar{K}N$ scattering data and its sub-threshold behavior, the two-body potentials are determined in a coupled-channel formalism including both elastic and inelastic channels. Three-body Faddeev equations are then solved by the use of the potentials, taking into account the coupling among the multi-channel interactions.

3. – Low-energy kaon-nucleon phenomenology

The measurement at the level of eV precision of kaonic hydrogen shift and width, together with the first measurement of kaonic deuterium will represent a breakthrough in the investigation of the low-energy kaon-nucleon interaction.

The three measurements on kaonic hydrogen performed at CERN and RAL [9] more than 20 years ago claimed to observe a signal with positive energy shift and hence an attractive strong interaction between antikaon and proton. This result was in striking contradiction with the low-energy scattering data extrapolated down to threshold, which showed a *repulsive* contribution of the strong interaction. The so-called "kaonic hydrogen puzzle" was born. The theoretical understanding of the observed claimed behaviour was indeed complicated by the existence, just below the threshold, of the $\Lambda(1405)$ resonance. No decent explanation of the "puzzle" could be achieved.

The observation of a faint but clean K_α signal by the KpX experiment at KEK [4] solved the longstanding mystery with a result which agrees with the scattering data. The low overall statistics did not allow, however, a real constraint for the theoretical description of the low-energy $\bar{K}N$ phenomenology.

The measurement of kaonic hydrogen at DAΦNE will allow to go beyond the KEK results and to perform a precision measurement of kaonic hydrogen and the first measurement on kaonic deuterium, drastically changing the present status of the low-energy $\bar{K}N$ phenomenology.

4. – Towards the understanding of the low-energy strong interaction dynamics

The QCD theory is regarded as the basic theory of the strong interaction. The theory possesses the important feature of asymptotic freedom: as the distance scale becomes smaller, or the momentum transfer becomes higher, the QCD coupling "constant" becomes weaker and the strength of the interaction diminishes. In this high-energy domain perturbative QCD is successfully applied. In the low-energy domain, the (running) QCD coupling constant becomes stronger and stronger and the theory exhibits the confinement of colour. The quarks and gluons are confined in the hadrons, which become the relevant degrees of freedom at low energies. At this point, perturbative QCD ceases to be a useful tool; at energies equal to or smaller than the scale of strong interactions (*simeq* 1GeV) one must simplify the whole theory. This is achieved by using models which approximate the low-energy region of QCD, being an admixture of QCD and phenomenology. A different approach is to perform lattice calculations, where the space-time continuum is replaced by discrete values of space and time.

At very low energies, however, a great simplification occurs. Below the resonance region ($E < M_\rho$) the hadronic spectrum contains only the pseudoscalar particles (π, K, η), whose interactions can be most easily understood from *global symmetry* considerations. Chiral symmetry holds if all quark masses were equal to zero. If quark masses were finite and equal, the exact unitary symmetry SU(3) is valid, which means multiplets of particles degenerate in mass. In the real world, quarks are massive and their masses are

different: $m_s > m_u \simeq m_d$. Thus, in the real world chiral symmetry is broken and the SU(3) symmetry is broken as well to the extent required to obtain the experimentally observed mass spectra.

We don't know, on a fundamental level, which is the origin of the symmetry breaking: its nature, to what extent it is broken and which are the breaking mechanisms. The measurement of kaonic atoms can contribute to investigate such primary problems.

4˙1. *The meson-nucleon sigma terms and the chiral symmetry breaking.* – There are, in principle, two sources of information about the SU(3) and chiral symmetry breaking. The first one is the fact that the entire mass of a pseudoscalar meson comes from the symmetry breaking mechanism. This, however, does not tell us much about the nature of the symmetry breaking interactions, except, when fitting the pseudoscalar mass spectrum, the magnitude of the free parameter in the symmetry violating piece of the strong interaction Hamiltonian.

By far more sensitive to the symmetry breaking mechanism are corrections to the so-called *low-energy* theorems. These theorems relate the symmetry breaking part of the total Hamiltonian to the scattering amplitude of massless particles: they would become exact in the limit where the pseudoscalar meson masses vanish and the axial vector currents are conserved. Consequently, important tests of theories of chiraly symmetry breaking come from the study of the low-energy theorems of meson-nucleon scattering, which just represent the "correction" for the real world to the exact relations valid for zero mass particles. In practice, this means calculating the *meson-nucleon sigma terms.*

The meson-nucleon sigma terms are quantities of relevant importance to the non-perturbative QCD and their main interest lies in the fact that they provide a measure of chiral symmetry breaking. They are important as well in connection with the strangeness content of the nucleon - see 4.2.

In order to define the meson-nucleon sigma terms consider the scattering process:

$$M_a(q) + N(p) \to M_b(q') + N(p') \tag{10}$$

with four momenta of the particles indicated in parenthesis while a and b are denoting the SU(3) indices of the mesons.

The meson-nucleon sigma term is the expectation value in the proton state $|p>$ of a double commutator of the symmetry breaking part of the strong interaction Hamiltonian, H_{SB} [10]:

$$\sigma_{MN}^{ba} = i < p|[Q_b^5, [Q_a^5, H_{SB}]]|p > \tag{11}$$

where $Q_{a,b}^5$ is the axial-vector charge.

The double commutator in eq. (11) - sigma commutator - is nothing else than the equal-time commutator of the axial vector current associated with Q_a^5, with its divergence $\delta_\mu A_a^\mu$ [10]. The partially conserved axial vector current (PCAC) hypothesis identifies then this divergence with the pseudoscalar meson field. In such a way, the sigma commutator in eq. (11) is replaced by the product of the two meson fields allowing one to connect the sigma term to the meson-nucleon scattering amplitude $T_{ba}(\nu, t, q^2, q'^2)$ and, finally, to obtain the low-energy theorem in the soft-meson limit: $q^2, q'^2 \to 0$, together with $\nu = 0$ and $t = 0$:

$$\sigma_{MN}^{ba} = -f_a f_b T_{ba}(0, 0, 0, 0,) \tag{12}$$

where the f's are the meson decay constants and the kinematic invariants of the process are defined by:

$$s = (q+p)^2, t = (q-q')^2, u = (q-p')^2, \nu = (s-u)/2M_N \tag{13}$$

The calculation of the sigma term from the scattering data requires an elaborate procedure. The problem is that the sigma term is *not* an observable by itself. One has then to introduce an "experimental" sigma term Σ_{MN} which can be related to the experimental meson-nucleon amplitudes. This can be done in a favored point of the (t, ν) plane, the so-called Cheng-Dashen (C-D) point ($t = 2\mu^2, \nu = 0$, μ being the meson mass).

The Cheng-Dashen point is on mass-shell but lies outside the physical meson-nucleon scattering region. Therefore, in order to obtain $\Sigma(2\mu^2)$ from the experimental amplitudes one has to extrapolate them to the C-D point, with a procedure commonly based on dispersion relations. The last step consists in calculating Σ in the zero momentum point, where the kinematic variables all vanish and the sigma term is defined by equation (12).

The pion-nucleon sigma term has been obtained by following this phenomenological approach. The same procedure might be used to evaluate the KN sigma terms (two - in correspondence with the isospin I=0 and I=1 states of the $\bar{K}N$ system). The procedure is shown schematically in Fig. 2 [11].

The situation is however much more difficult than in the pion case. On the experimental side this is due to the poor bulk of $K^{\pm}N$ scattering data, while on the theoretical side complications arise from the fact that there are open channels below threshold, from the presence of the $\Lambda(1405)$ and from uncertainties in the phenomenological procedure.

The result is that presently no precise determination of KN sigma terms does exist. One recent updated analysis of meson-nucleon sigma terms in the perturbative chiral quark model is given in [12].

In this framework, the DEAR/SIDDHARTA results will not only contribute to the extraction of the scattering amplitude at threshold, but , hopefully, will place strong constraint on the extrapolations to zero energy which are required in any analysis of scattering data. In fact, the s-wave K^-N amplitudes will be determined more accurately, below and above threshold. This will provide a tighter constraint on the p-wave parameters from experimental data and, eventually, reduce the uncertainty in the phenomenological procedure used to calculate the sigma terms.

4·2. *Strangeness content of the nucleon.* – Spin-dependent deep inelastic scattering experiments have demonstrated that nucleon structure functions cannot be fully described by valence quark models based on the SU(2) scheme. A strange quark fraction in the nucleon is the most probable hypothesis. While several parity-violating electron scattering experiments are either under way or planned, another way to look for the strangeness content of the nucleon is represented by the determination of the meson-nucleon sigma terms. Indeed, the SU(3) structure of the nucleon appears more explicitly in quantities associated with chiral symmetry breaking.

The complementary approach of using the meson-nucleon sigma terms to determine the strangeness content of the nucleon has its source in the fact that the symmetry breaking Hamiltonian, H_{SB} - to which sigma terms are directly connected, is the quark mass term of the total Hamiltonian:

$$H_{SB} = m_u \bar{u}u + m_d \bar{d}d + m_s \bar{s}s \tag{14}$$

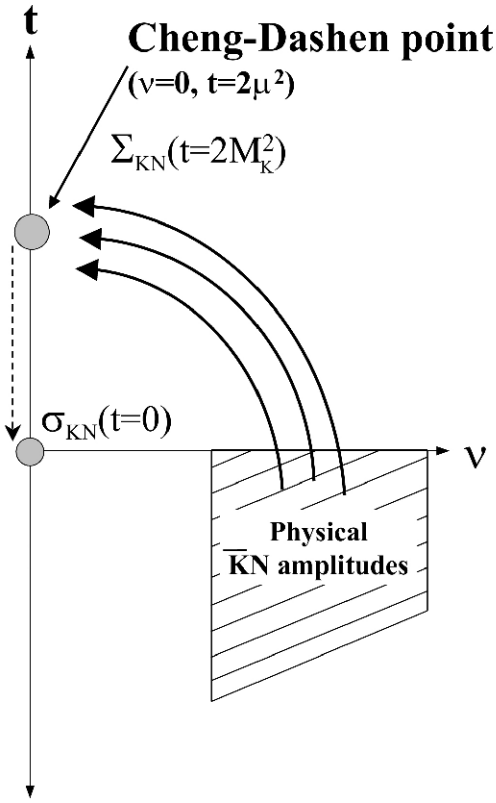

Fig. 2. – *The determination of the sigma term from the experiment*

$$\simeq \frac{1}{3}(m_s + 2\bar{m})(\bar{u}u + \bar{d}d + \bar{s}s) - \frac{1}{3}(m_s - \bar{m})((\bar{u}u + \bar{d}d - 2\bar{s}s) = H_0 + H_8 \tag{15}$$

where $\bar{m} = m_u = m_d$ assuming isospin invariance. The singlet term H_0 preserves the SU(3) symmetry while the octet term H_8 breaks it.

One can then define the sigma terms through quark masses and quark scalar densities [13]:

$$\sigma_{KN}^{(1)} = \frac{1}{2}(\bar{m} + m_s) < p|\bar{u}u + \bar{s}s|p > \tag{16}$$

$$\sigma_{KN}^{(0)} = \frac{1}{2}(\bar{m} + m_s) < p| - \bar{u}u + 2\bar{d}d + \bar{s}s|p > \tag{17}$$

$$\sigma'_{KN} = \frac{1}{4}(3\sigma^{(1)}_{KN} + \sigma^{(0)}_{KN}) \tag{18}$$

$$\sigma_{\pi N} = \bar{m} < p|\bar{u}u + \bar{d}d|p > \tag{19}$$

The fraction y of strange quark content of the proton is defined as:

$$y = \frac{2 < p|\bar{s}s|p >}{< p|\bar{u}u + \bar{d}d|p >} \tag{20}$$

This quantity can be expressed through the sigma terms previously defined:

$$y = \frac{4\bar{m}}{\bar{m} + m_s}\frac{\sigma'_{KN}}{\sigma_{\pi N}} - 1. \tag{21}$$

It turns out that y is particularly sensitive to σ_{KN} [14]. Therefore, DEAR/SIDDHARTA can contribute to a better determination of the strangeness content of the nucleon.

5. – The DEAR setup on DAΦNE

The principle of the DEAR experiment is straightforward: low momentum negative kaons produced in the decay of the ϕ-mesons at DAΦNE leave the thin-wall beam pipe, are degraded in energy to a few MeV, enter a gaseous target through a thin window and are finally stopped in the gas. The stopped kaons are captured in an outer orbit of the gaseous atoms, thus forming the exotic kaonic atoms. The kaons cascade down and some of them will reach the ground state emitting X rays. The energy of the X rays emitted in these transitions is measured with a CCD (Charge-Coupled Device) detector system [15].

Fig. 2 shows a schematic of the DEAR experimental setup. The cylindrical cryogenic target cell had a diameter of 12.5 cm and a height of 14 cm. Special care was taken to avoid materials with fluorescence X rays in the region of the kaonic atoms transitions. Therefore, a light target was chosen, made only of aluminium (top-plate and entrance ring), kapton (side wall and entrance window) and a support structure in fiberglass. A picture of the target is shown in Fig. 3.

Two measurements were performed: tha kaonic nitrogen and kaonic hydrogen ones - results of which will be presented in Section 6. The target was operated:

- for kaonic nitrogen at 1.5 bar and 120 K, corresponding to a density of $\rho = 3.4\rho_{NTP}$;
- for kaonic hydrogen at 2 bar and 25 K, corresponding to a density of 2.1 g/l.

16 CCD detector chips (Marconi Applied Technologies, CCD55-30) with a total area of 116 cm^2 were placed around the cryogenic target cell. Each chip has 1242 x 1152 pixels with a pixel size of 22.5 μm x 22.5 μm and a depletion depth of about 30 μm. The working temperature was stabilized at 165 K to achieve the energy resolution of 150 eV at 6 keV with a readout every 90 seconds. The CCD front-end electronics and controls, and the data acquisition system, were specially made for this experiment [16].

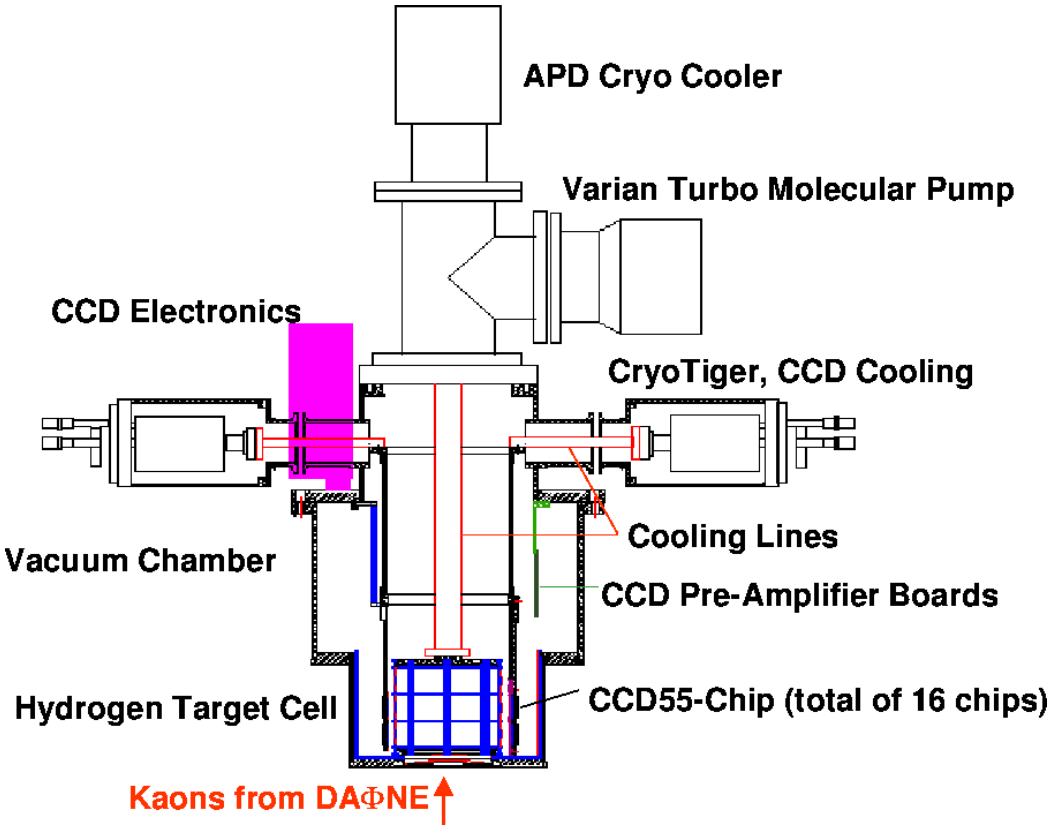

Fig. 3. – *Schematic representation of the DEAR setup*

6. – Experimental results on kaonic atoms

The DEAR experiment was installed at DAΦNE at the beginning of 1999. It took data for periods of 2-3 months/year, sharing the DAΦNE beam with the KLOE experiment [17].

After a period of machine and setup optimization, with a continuous increase of luminosity and decrease of background (optics and shielding), in 2002 DEAR performed two kind of kaonic atoms measurements: the kaonic nitrogen and the kaonic hydrogen one.

In what follows, the results of these measurements are presented.

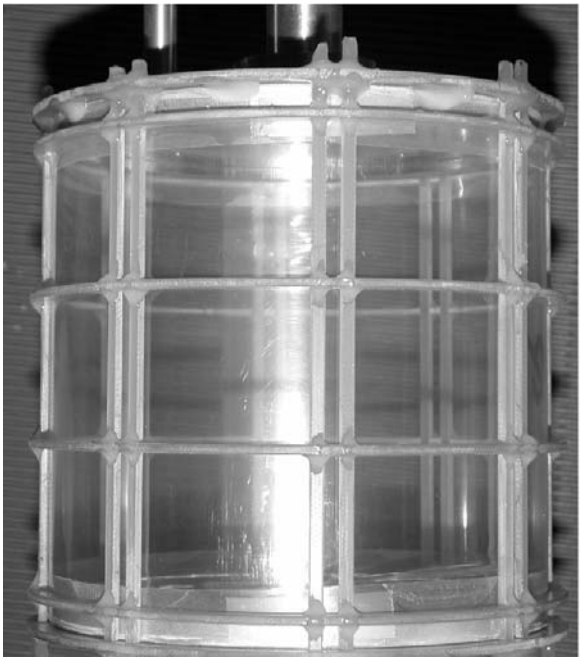

Fig. 4. – *The DEAR target cell, made in kapton, with fiberglass reinforcements.*

6˙1. *Kaonic nitrogen results.* – The measurement of kaonic nitrogen had multiple tasks and deliverables:

- a feasibility study of the DEAR technique to produce and detect kaonic atoms at DAΦNE;
- study of the machine background and of the setup performance and the optimization of the signal to background ratio;
- the first measurement of kaonic nitrogen transition yields.

Understanding the atomic cascade processes in kaonic nitrogen is especially important due to the possible role of this exotic atom for a precise determination of the charged kaon mass - still an open problem [18]. Even if X-ray transitions were measured for many kaonic atoms [19] no results have been published for nitrogen, apart the preliminary DEAR ones [18].

For the kaonic nitrogen transition yields measurement, DEAR used a cryogenic and pressurized gaseous target (see Section 5), because the yield of kaonic nitrogen transitions in these conditions is high enough to allow a fast feedback. Data using the nitrogen target were taken for about one month (October 2002), leading to the optimization of the setup performance in terms of signal/background ratio. A total of 17.4 pb^{-1} of integrated luminosity was collected, from which 10.8 pb^{-1} taken in stable conditions were selected for the analysis of the energy spectrum.

In fig. 4 the kaonic nitrogen spectrum after subtraction of the continuous background is shown.

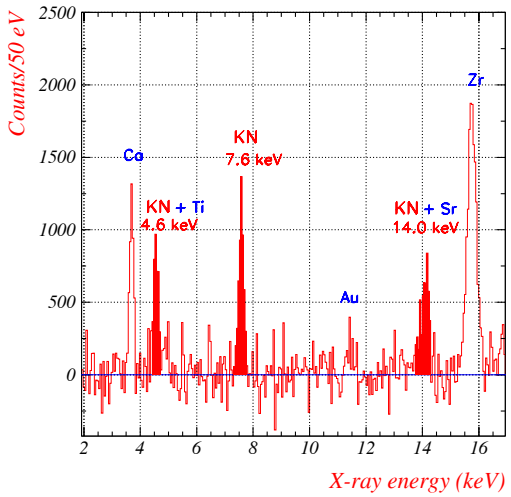

Fig. 5. – *The kaonic nitrogen continuous background subtracted spectrum.*

Three kaonic nitrogen X-ray lines are well indentified. The $n = 6 \to 5$ kaonic nitrogen transition peak at 7.6 keV is clearly seen. The transition lines $n = 7 \to 6$ and $n = 5 \to 4$ at 4.6 and 14.0 keV are overlapped with the Ti-K_α and Sr-K_α lines, respectively.

In order to estimate the transition yields, Monte Carlo calculations which took into account the kaon stopping efficiency in the target gas, the X-ray absorption in gas and target windows and the CCD quantum efficiency, were performed.

The determined yields are [20]:

1. for the $n = 7 \to 6$ transition:

$$41.5 \pm 8.7(stat.) \pm 4.1(syst.)\% \tag{22}$$

2. for the $n = 6 \to 5$ transition:

$$55.0 \pm 3.9(stat.) \pm 5.5(syst.)\% \tag{23}$$

3. for the $n = 5 \to 4$ transition:

$$57.4 \pm 15.2(stat.) \pm 5.7(syst.)\% \tag{24}$$

The precision in the position of the $n = 6 \to 5$ energy transition value: 7.558 ± 0.005 keV, could be used to evaluate the charged kaon mass from the first order of the Klein-Gordon equation using a point-like nucleus, which resulted in:

$$M_{K^-} = 493.884 \pm 0.314\ MeV \tag{25}$$

which represents an improvement by one order of magnitude in precision with respect to the DEAR preliminary results [18].

6·2. *Kaonic hydrogen results.* – In the period November-December 2002 the kaonic hydrogen measurement was performed - just after the kaonic nitrogen one. Data for 58.4 pb^{-1} were collected in this period. At the end of the period, a background measurement with separated electron and positron beams and intentionally high X-ray background was performed (no-collision spectrum).

Two independent analyses were performed in order to obtain the kaonic hydrogen lines from which to extract the strong interaction shift and width. In both analyses Voigt functions with Gaussians for the detector resolution were used for the kaonic hydrogen lines. Fit parameters were the intensities of K_α, K_β and K_γ, the energy of K_α and the Lorentzian width for K_α, equal for all the K-transitions, obviously.

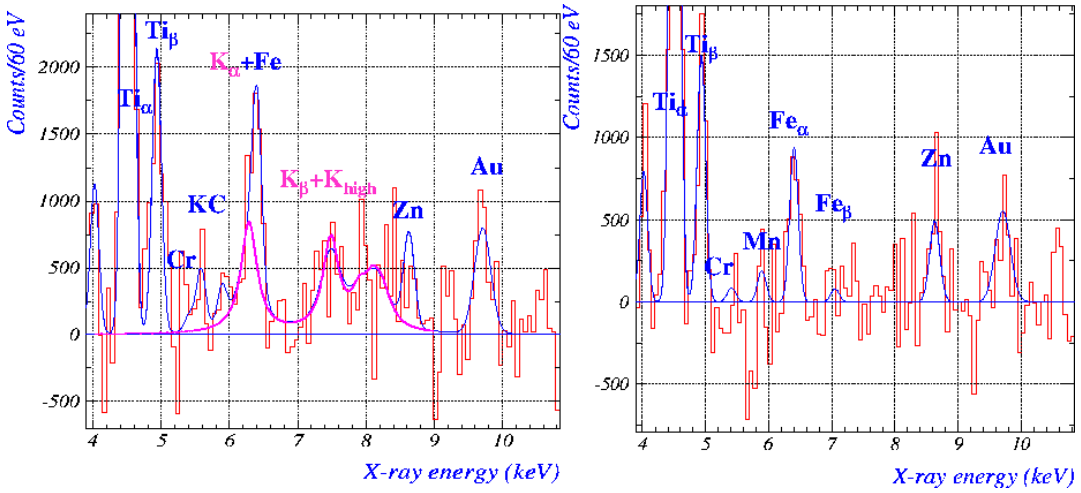

Fig. 6. – *The kaonic hydrogen (left) and no-collision (right) continuous background subtracted spectra. The kaonic hydrogen transitions are visible in the kaonic hydrogen spectrum. The electronic transition are due to setup materials excited by the background particles.*

In one of the analyses a simultaneous fit of the kaonic hydrogen and no-collision spectra was performed. The same function fitted the continuous background and the electronic peaks, apart a normalization factor. The energy region corresponding to K_{high} (higher than K_γ) was excluded from the fit, since the lines in this region could not be distinguished by the fit and no precise information exists for the relative yields. It was estimated by Monte Carlo that the systematic error introduced by this cut is at the level of the eV and was included in the final result. The two spectra (kaonic hydrogen and no-collision) with the continuous background subtracted are shown in Fig. 5.

Apart from kaonic hydrogen transitions, there are lines coming from the excitation of materials (electronic X-ray transitions) present in the setup. A thin Titanium foil was placed on the upper wall of the target cell for calibration purpose. Other materials -

Iron, Zinc, etc. - are present in very small quantities (ppm) in the materials of the setup.

In the second analysis the kaonic hydrogen spectrum was analyzed together with a spectrum built as a sum of the kaonic nitrogen one and a subset (low CCD occupancy) of the no-collision one. A constrained fit based on the ratios of the electronic transitions in the two spectra, was then performed. The K_{high} region was dealt with analogously the first analysis. Some tests of the stability of the results and of the systematic errors were done by considering various cascade models of kaonic hydrogen transitions giving the transition yields [21].

The "pure" kaonic hydrogen spectrum with the background (continuous and structured) subtracted is shown in Fig. 6.

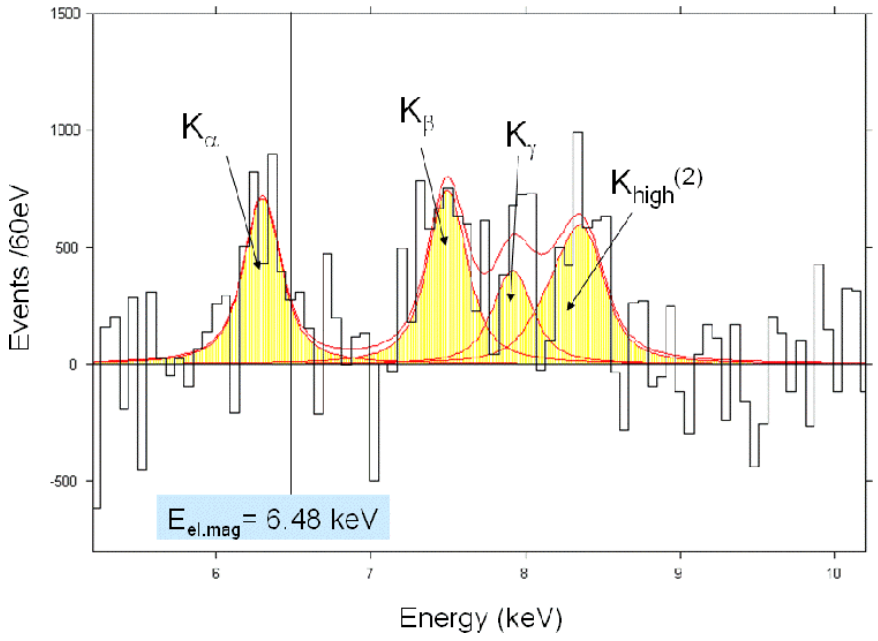

Fig. 7. – *The kaonic hydrogen background (continuous and structured) subtracted spectrum*

The weighted averages of the two analyses for the shift and width of the $1s$ ground state of kaonic hydrogen are:

$$\epsilon = -193 \pm 37(stat.) \pm 6(syst.)\ eV \tag{26}$$

$$\Gamma = 249 \pm 111(stat.) \pm 39(syst.)\ eV \tag{27}$$

These results confirm the KEK values and the repulsive character of the $K^- p$ interaction at threshold. They differ however significantly from the KEK results (eq. (3) and (4)) in two aspects: the errors are a factor 2-3 smaller; moreover, DEAR was able, for the first time, to obtain a full pattern of the K-series lines of kaonic hydrogen: K_α, K_β and K_γ were clearly identified with an overall statistics significance of 6.2 σ.

7. – Future perspectives: the SIDDHARTA experiment

DEAR has performed (Section 6) the most precise measurement of kaonic hydrogen; the precision which was achieved, however, is at the level of tens of eV, whilst the goal of a precision measurement should push this precision in the eV range. The DEAR precision was limited by a signal/background ratio of about 1/70. In order to go beyond this ratio a jump of quality is necessary. Consequently, an accurate study of the background sources present at DAΦNE was re-done. The background includes two main sources:

- synchronous background: coming together with the K^- - related to the ϕ-decay process; it can be defined hadronic background;
- asynchronous background: final products of electromagnetic showers in the machine pipe and in the setup materials originated by particles lost from primary circulating beams either due to the interaction of particles in the same bunch (Touschek effect) or due to the interaction with the residual gas.

Accurate studies performed by DEAR showed that the main background source in DAΦNE is of the second type, which shows the way to reduce it. A fast trigger correlated to the negative kaon entrance in the target would cut the main part of the asynchronous background. This was not possible in DEAR, which used as X-ray detector the CCDs - which are slow devices.

A new detector was then identified, which preserves all the good features of the CCDs (resolution, linearity and stability) but is fast enough to supply a trigger at the level of one μs. It was estimated to cut in such way the background present in DEAR by 2-3 orders of magnitude. The detector is the newly developed large area Silicon Drift Detector (SDD), based on which a new experiment, which continues the DEAR scientific line, was born. The new experiment is SIDDHARTA (SIlicon Drift Detector for Hadronic Atom Research by Timing Application) [3].

Presently, construction and testing of the SDD detectors and of the electronics and mechanical structures is in progress. The setup will be installed at DAΦNE in 2006 and start taking data for kaonic hydrogen and kaonic deuterium.

In the next Sections, a brief description of the SDD detector and of the tests performed with a preliminary setup, are given.

7˙1. *Large Area Silicon Drift Detectors.* – The Silicon Drift Detectors (SDD) were developed as position sensitive detectors which operate in a manner analogous to gas drift detectors [22]. Recently, SDD started to be used as X-ray detectors in X-ray fluorescence spectroscopy, electron miniprobe analysis systems and synchrotron light application. SDDs with sensitive areas of up to 10 mm^2 are commercially available since several years. The typical energy resolution is better than 140 eV (FWHM) at 5.9 keV and -20 degrees centigrade. The outstanding property of a SDD is its extremely small anode capacitance, which is independent of the active area. Thus, the electronics noise is very low, and much shorter shaping times than for PIN diodes or Si(Li) detectors can be used.

The two main noise contributions of a detector are the leakage current and the capacitance. The equivalent noise charge increases linearly with the capacitance but only with the square root of the leakage current, which is correlated to the temperature. The leakage current depends on the detector area, but due to the drift principle the anode size and thus the capacitance is constant. Then, it can be expected that SDDs with much

more han 10 mm^2 area still have a good energy resolution. Taking then into account the small shaping time, a trigger application of large area SDD as an X-ray detector, with a time window limited by its active area (drift time) can be envisaged. One of the ideal applications of such a triggered large area SDD detector is the measurement of exotic atoms X-ray transitions . The X-ray energies, ranging from few to tens of keV, are well in the range of maximum efficiency of SDDs, while a trigger based on a time-window of the order of μs was demonstrated by Monte Carlo simulation to dramatically reduce the background and to allow a precision measurement of exotic atom transitions. The trigger in this case is given by the specific process which generated the K^- at DAΦNE, namely a back-to-back reaction of the type:

$$\phi \to K^+K^-. \tag{28}$$

A program to develop such kind of large area (1 cm^2) triggerable SDD detectors, with integrated electronics (JFET) on it, started as a collaboration of MPI (Max-Planck Institut), PNSensors, Politecnico di Milano and LNF.

7˙2. *Experimental requests.* – The experimental requests put forward for the new large area triggerable SDD detectors with integrated JFET and equipped with a newly under development electronics, to be used for X-ray measurements, are:

- energy range of interest: 0.5 - 20/40 keV, with a selectable gain;
- capability to operate under mainly high energy events (background), with an event rate of the order of KHz/channel;
- energy resolution: better than 140 eV (FWHM) at 6 keV of energy;
- stability and linearity better than 10^{-4} for a precision measurement;
- trigger at the level of 1μs.

Total number of channels to be processed: 200 (for a total area of 200 cm^2); eventual use of multiplexing - to be optimized. This is the first application in which SDDs are used with a trigger system.

7˙3. *Preliminary measurements.* –

7˙3.1. BTF tests with a 7 chips array prototype. Preliminary tests were performed at the Beam Test Facility (BTF) at Frascati with a prototype SDDs array: 7 chips of 5mm^2 each. A trigger was implemented and tested with a time window of 1μs. A synchronous (with BTF beam) as well as an asynchronous background (Fe and Sr sources) were implemented and it was checked that the rejection factor is in agreement with what expected. In Fig. 8 the results of the tests with the trigger are shown [3].

7˙3.2. Preliminary laboratory tests with a 30 mm^2 chip. Preliminary measurements in laboratory with a SDD chip of 30 mm^2, shown in Fig. 9, were performed in June 2004. The chip was cooled at -40^0 C (by the use of a cryotiger) and a shaping time of 0,75 μs was used. The energy resolution measured was of 139 eV (FWHM) at 5.9 keV, as seen in Fig. 10.

The tests will be continued with the trigger measurements on the BTF.

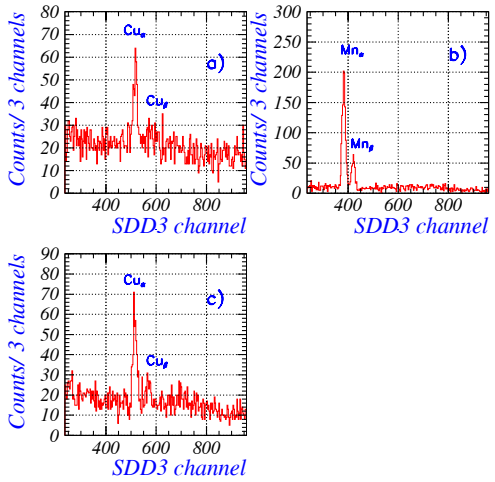

Fig. 8. – *a) No trigger, only BTF signal which excites the Cu-line, 5 Hz rate - 16 hours of DAQ; b) No trigger, 60 Hz, BTF signal (Cu) covered by Sr plus Fe radioactive sources as asynchronous background - 20 minutes DAQ; c) same as b) but trigger on, 5Hz as in a) - 16 hours of DAQ.*

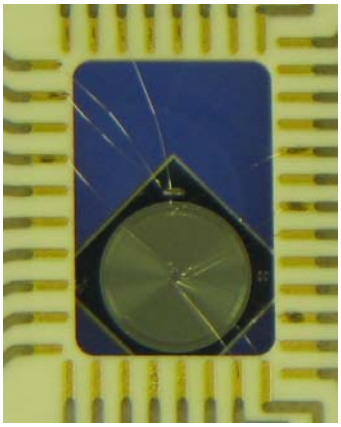

Fig. 9. – *The 30 mm^2 SDD chip used for testing in the laboratory.*

7˙4. *The 1 cm^2 SDD chip.* – The 1 cm^2 SDD chip to be used in the SIDDHARTA experiment is under production, at PNSensors (Germany). The electronics is under development. The SDD layout on the readout side is shown in Fig. 11.

The sensitive area per chip (containing 3 SDDs) is 3 cm^2; the SDDs are squared with round corners. The maximum diagonal drift length is 5.15 mm (centerlines) and 6.4 mm (diagonal).

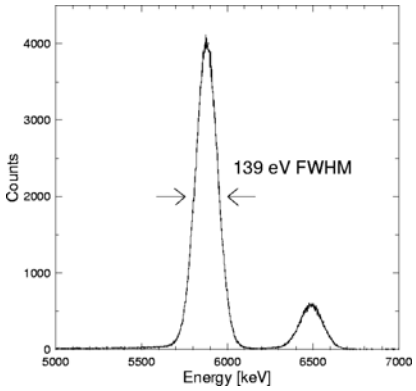

Fig. 10. – *The X-ray spectrum from an Iron source as measured in the laboratory with the 30 mm^2 SDD chip.*

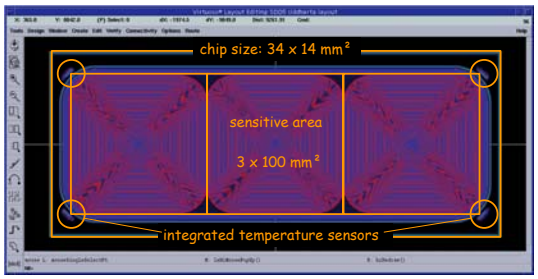

Fig. 11. – *SDD layout on the readout side*

7˙5. *The SIDDHARTA setup.* – There are two preliminary SIDDHARTA setup under studies, which are shown in Fig 12 and 13.

The first version is DEAR-like, while the second one is toroidal, around the beam pipe. Detailed Monte Carlo studies were performed in order to optimize all the experimental requests for a precision measurement.

The kaonic hydrogen simulated spectrum obtainable for about 100 pb^{-1} of integrated luminosity in SIDDHARTA, with a signal/background ratio of about 4/1 is shown in Fig. 14.

With such a spectrum a precision at the level of eV for kaonic hydrogen is reachable.

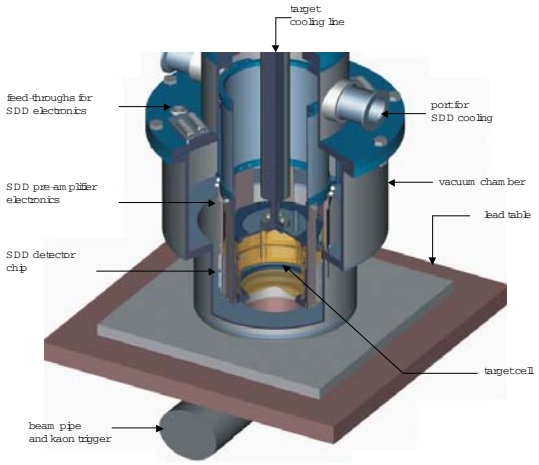

Fig. 12. – *SIDDHARTA preliminary setup - version 1*

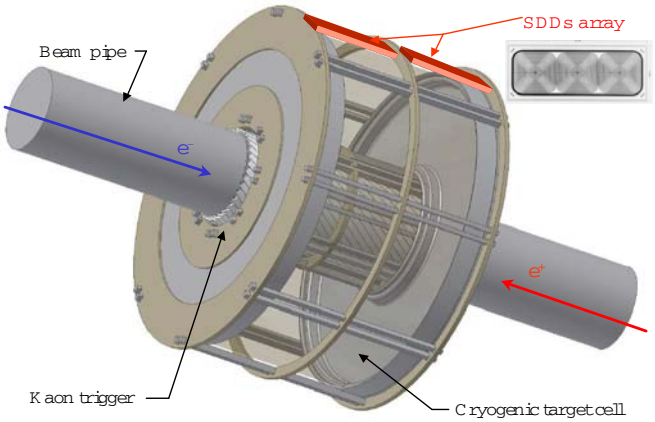

Fig. 13. – *SIDDHARTA preliminary setup - version 2*

8. – Conclusions

DAΦNE has unique features as kaon source, which is intrinsically clean and of low momentum, a situation unattainable with fixed target machines, especially suitable for kaonic atom research.

The DEAR/SIDDHARTA experiments combine the newly available techniques with the good kaon beam quality to initiate a renaissance in the investigation of low-energy

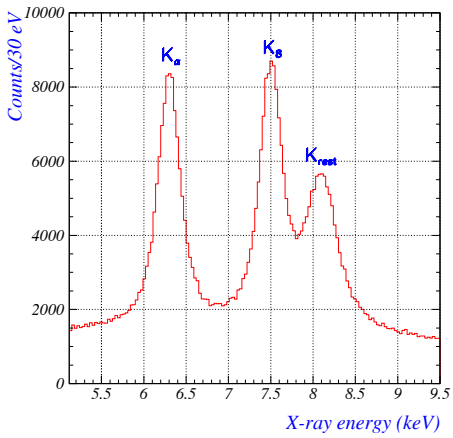

Fig. 14. – *The kaonic hydrogen Monte Carlo simulated spectrum for 100 pb^{-1} of integrated luminosity in SIDDHARTA*

kaon-nucleon interaction.

DEAR has performed the most precise measurement of kaonic hydrogen; the eV precision measurement of the strong interaction shift and width of the fundamental level in kaonic hydrogen will be performed by SIDDHARTA. The first measurement of kaonic deuterium is as well planned. These results will open new windows in the study of the kaon-nucleon interaction, in particular chiral symmetry breaking in the strangeness sector, via the determination of the kaon nucleon sigma terms.

The measurement of kaonic helium, feasible in SIDDHARTA, will allow to study the behaviour of the subthreshold resonance $\Lambda(1405)$ in nuclear matter. Other light kaonic atoms can be studied in SIDDHARTA as well.

DAΦNE proves to be a real and ideal "kaonic atoms" factory.

REFERENCES

[1] G. Vignola, Proc. of the "5th European Particle Accelerator Conference", Sitges (Barcelona), Eds. S. Myres *et al.*, Institute of Physics Publishing, Bristol and Philadelphia (1996) 22.
[2] S. Bianco *et al.*, Rivista del Nuovo Cimento **22**, No. 11 (1999) 1.
[3] J. Zmeskal, SIDDHARTA Technical Note IR-2 (2003); C. Curceanu, (Petrascu), SIDDHARTA Technical Note IR-3 (2003).
[4] M. Iwasaki *et al.*, Phys. Rev. Lett **78** (1997) 3067;
T.M. Ito *et al.*, Phys. Rev. **A58** (1998) 2366.
[5] S. Deser *et al.*, Phys. Rev. **96** (1954) 774;
T.L. Truemann, Nucl. Phys. **26** (1961) 57;
A. Deloff, Phys. Rev. **C13** (1976) 730.
[6] U.-G. Meissner, U. Raha and A. Rusetsky, E. Phys. J. **C35** (2004) 349.
[7] J. Gasser, Mini-proceedings of the 4th International Workshop on *Chiral Dynamics 2003: Theory and Experiment*, Bonn 2003, edited by U.-G. Meissner, H.-W. Hammer and A. Wirzba, p.126.

[8] J. Gasser, in Frascati Physics Series, Proceedings of the *DAFNE 2004: Physics at meson factories*, Frascati 2004 - to appear.
[9] J.D. Davies *et al.*, Phys. Lett. **83** (1979) 55;
M. Izycki *et al.*, Z. Phys. **A297** (1980) 11;
P.M. Bird*et al.*, Nucl. Phys. **A404** (1983) 482.
[10] E. Reya, Rev. Mod. Phys. **46** (1974) 545;
H. Pagels, Phys. Rep. **16** (1975) 219.
[11] C. Guaraldo, Physics and detectors for DAΦNE, Frascati Physics Series **16** (1999) 643.
[12] T. Inoue, V. Lyubovitskij, T. Gutsche, A. Faessler, Phys. Rev. **C69** (2004) 035207.
[13] J.F. Gunion, P.C. McNamee, M.D. Scadron, Nucl. Phys. **B123** (1977) 445.
[14] R.L. Jaffe and C.L. Korpa, Comments Nucl. Part. Phys. **17** (19876) 163.
[15] J.-P. Egger, D. Chatellard, E. Jeannet, Part. World. **3** (1993) 139.
[16] M. Iliescu *et al.*, Nucl. Instr. Meth., in preparation.
[17] The KLOE Collaboration, LNF-93/002 (IR), (1993)
[18] G. Beer *et al.*, Phys. Lett. **B535** (2002) 52.
[19] C.E. Wiegand, G.L. Godfrey, Phys. Rev. **A9** (1974) 2282;
C.J. Batty, Sov. J. Part. Nucl. **13** (1982) 71.
[20] T. Ishiwatari *et al.*, Phys. Lett. **593** (2004) 48.
[21] T. Jensen, DEAR Technical Note IR-45 (2003).
[22] E. Gatti, P.Rehak, Nucl. Instr. and Meth. **225** (1984) 608;
E. Gatti, P.Rehak, Nucl. Instr. and Meth. **A235** (1985) 224.